AlGaN Schottky diodes for detector applications in the UV wavelength range

Abstract— **We report on the use of TCAD simulations to optimize AlGaN UV-detectors for space applications and advanced EUV lithography tools. (i) High dark current in present AlGaN Schottky diodes is explained by means of the Thin Surface Barrier model. (ii) This model and AlGaN material properties were implemented in TCAD software and verified with experimental results, facilitating future technology development. (iii) Key issues in technology development were identified and experimentally verified: reducing surface defects is shown to result in order-of-magnitude dark current reduction. (iv) A full semi-transparent Schottky contact is shown to provide a good compromise between low leakage and sufficient photocurrent.**

Keywords— **Ultraviolet, Detector, Imager, AlGaN, Solar Orbiter, EUV lithography.**

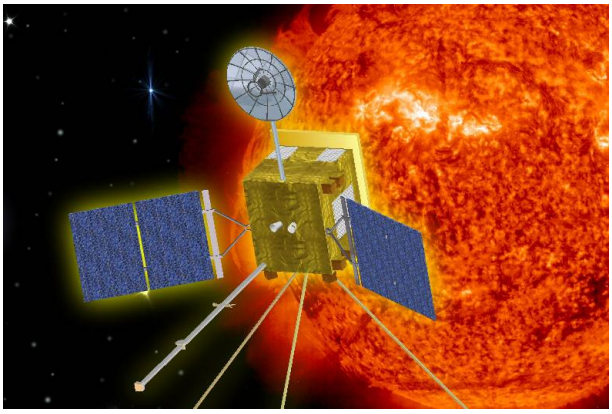

Fig. 1
Artist's impression of ESA's Solar Orbiter satellite, planned launch in 2015 [1].

I. Introduction

ESA'S Solar Obiter (planned launch in 2015) is intended to brave the fierce heat and carry its telescopes to just one-fifth of the Earth's distance from the Sun, where sunlight will be twenty-five times more intense than we feel it. While the spacecraft endures the powerful bursts of atomic particles from explosions in the solar atmosphere, its instruments will provide scientists with detailed images of this frenzied spectacle [1]. The Solar Orbiter is intended to carry six imagers for extreme-UV (EUV) wavelengths ($\lambda = 4 - 150\ nm$). A high spatial resolution, high sensitivity to EUV, solar blindness (insensitivity to visual and IR wavelengths), fast temporal cadence as well as total system weight, long-term stability and sensitivity to contamination are key specifications for these imagers [2], [3].

Current solar atmospheric studies from the SOHO and TRACE satellites (launched in 1995 and 1998 respectively) show that improved EUV observations would be of tremendous value to future advances in the field. However, silicon based EUV imagers onboard these spacecraft exhibit limitations inherent to their actual material and technology [2]. The optical filters suffer from severe degradation in space, making calibration difficult. The used Multi-Channel-Plate amplifier requires a high-voltage supply and inherently has an uncertain gain and signal saturation [4]. Finally, ionizing radiation degrades the silicon CCD by creating charge traps [5]. The CCD is cooled to -80°C to reduce radiation damage, hereby requiring a heavy cooling system. The cooled detector acts as a cold trap for contaminants, leading to a reduction in sensitivity.

The development of EUV sensitive detectors is also an enabler for future EUV-lithography tools. While EUV mirrors and lenses are being fabricated in high quality and sources are getting optimized, the existing prototype tools are suffering from the lack of detectors to characterize the EUV light from the source to the mask. Conventional silicon based EUV detectors suffer from the applied radiation and show a tendency to degrade in time. Their sensitivity to visual wavelenghts increases the noise on the signal.

The use of III-N wide-bandgap semiconductors like GalliumNitride (GaN), AluminumNitride (AlN), or AluminumGalliumNitride ($Al_xGa_{1-x}N$) in an active pixel sensor could surmount a lot of these difficulties. Their compact crystal lattice results in higher resilience against ionizing radiation [6], eliminating the need for cooling hardware [2]. However, the most important property of these materials is their solar blindness: the wide bandgap ($E_g = 3.4\ eV$ for GaN; 6.2 eV for AlN) makes these materials insensitive to the visual and IR light. Photons with an energy smaller than the bandgap are not absorbed. This significantly lowers the number of optical filters needed, resulting in fewer calibration problems. The largest drawback however, is that AlGaN technology is still in a prototype phase, compared to the fully mature silicon CCD [7].

The goal of this paper is therefore to investigate UV-detectors based on III-N semiconductors and to offer ways to increase their performance. Taking into account that the devices are limited by the Johnson noise, the single pixel performance can be determined by the specific detectivity D^* [8]. In a first iteration, this figure of merit

can be interpreted as a signal-to-noise ratio, determined as the ratio between the pixel's photo current (current under illumination) and its dark current:

$$S/N = I_{photo}/I_{dark} \quad (1)$$

Maximizing this S/N can be done by (i) increasing the photocurrent or (ii) reducing the dark current. As the quantum-efficiency (QE) of present III-N diodes is already at about 20 percent [9], [10], [11], only a modest factor of 5 can be realized by increasing the photocurrent. Diminishing the dark current potentially has a much larger influence, as it can be decreased by several orders of magnitude.

This paper is structured as follows. Section II-A introduces a theoretical model for the anomalously high dark currents in present III-N Schottky diodes. A customized TCAD simulator (Technology Computer-Aided Design) is combined with semi-classical quantum mechanical calculations and I-V measurements. Section II-B identifies key-issues in technology development and formulates processing-related opportunities to lower the dark current. Section II-C elaborates on experimental results, supporting the previous exposition. Section III presents an analysis of different detector structures, in terms of both photo and dark current.

II. Dark current

Thanks to their photovoltaic capabilities, Schottky diodes are considered the preferred devices for pixels in future EUV-imagers. The lack of high quality p-type AlGaN makes pn-diodes less favorable structures.

A. Theoretical model

A.1 Thermionic Emission (TE)

Schottky diodes formed on GaN and related materials suffer from anomalously high leakage current (or dark current) under reverse bias. Initial efforts to explain this behavior have concentrated on the Schottky barrier height and its metal dependence based on the thermionic emission theory (TE). The Schottky diode then behaves much like an ordinary pn-diode: the leakage current under reverse bias (illustrated in fig. 2a) is due to thermally excited electrons jumping over the Schottky barrier [12]. The I-V characteristic is a constant reverse current, combined with an exponential forward current (i.f.o. applied voltage)

Fig. 3 shows the I-V characteristic of two typical GaN Schottky diode (symbols). When comparing this I-V curve to the one predicted by the above TE theory, a fitting error of about 10 orders of magnitude is found (at -10V). From this, it is already clear that the TE theory does not give an adequate description of the current mechanism in the measured Schottky diodes.

A.2 (Thermionic-)Field Emission (TFE/FE)

An alternative theoretical model that could explain the high leakage current, is based on tunneling through the potential barrier. A detailed description of this theory was given in [13]. Under certain circumstances, electrons with an energy smaller than Φ_B can tunnel through the Schottky barrier. This can happen either at an energy equal to the Fermi level E_F of the metal (Field Emission - FE) or at a higher energy (Thermionic-Field Emission - TFE). Both mechanisms are schematically shown in fig. 2a. This effect was implemented in a TCAD simulator (Sentaurus, [14]) and the resulting current numerically calculated. The I-V curve (also in fig. 3) lies already closer to the experimental curves and exhibits a similar voltage dependence. It is however still about 6 orders of magnitude too low. The simulation assumes $\Phi_B = 1.2\ eV$, GaN doping level $N_d = 1.10^{17} cm^{-3}$. A better fit would be obtained by increasing N_d, but this would require unrealistic values for this parameter [15].

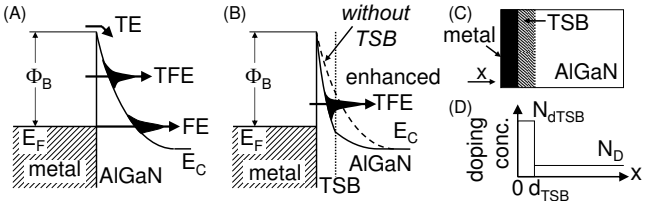

Fig. 2

Current transport mechanisms in the various theoretical models discussed (a,b) and schematic representation of the TSB model (c,d), after [17].

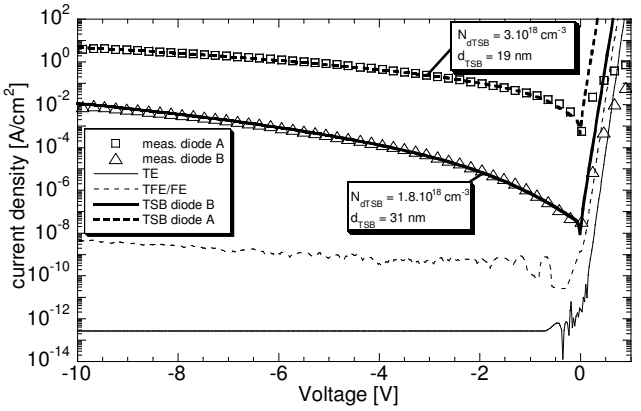

Fig. 3

Measured I-V characteristic for two GaN Schottky diodes and fits with Thermionic Emission (TE), (Thermionic-)Field Emission (TFE/FE) and Thin Surface Barrier model (TSB).

A.3 Thin Surface Barrier Model (TSB-model)

Hasegawa *et al.* [16] have proposed the Thin Surface Barrier (TSB) model to explain the observed I-V behavior in GaN. This model is represented schematically in fig. 2b-d. It assumes a thin layer underneath the Schottky contact, with a high density of defects or impurities, which act as dopants. The presence of these defects makes the Schottky barrier thinner. As a result, the tunneling current through

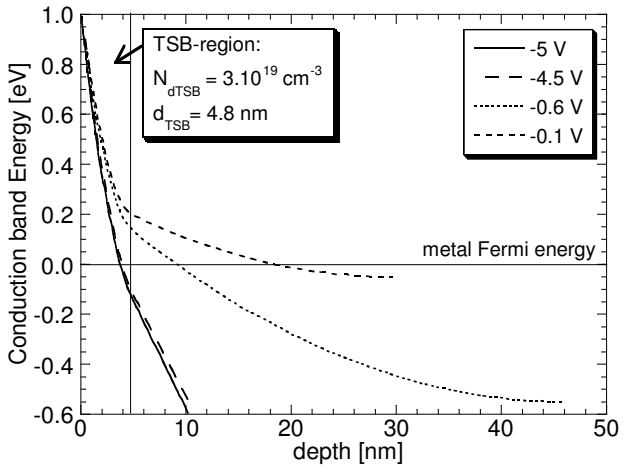

Fig. 4
Calculated Schottky barrier profile (AlGaN conduction band) for different bias conditions.

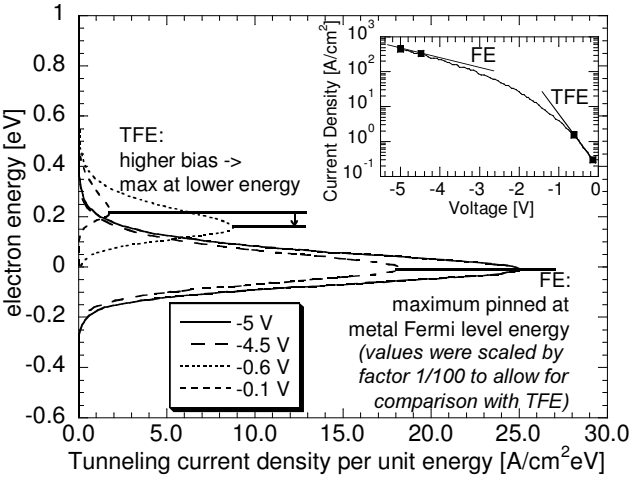

Fig. 5
Tunneling current in function of the electron energy for different bias conditions and I-V curve (inset).

TFE or FE mechanisms is drastically increased.

Because the tunneling probability is exponentially dependant on the thickness of the Schottky barrier, the leakage current increases by several orders of magnitude. The analytical description of this model is based on several approximations and has been reported in [16]. It will not be further elaborated here. Essentially, the result is a piecewise expression for the leakage current in function of 4 parameters: the Schottky barrier height $\Phi_B[eV]$, the effective defect concentration in the TSB-layer $N_{dTSB}[cm^{-3}]$, the thickness of the TSB-layer $d_{TSB}[nm]$ and the doping concentration of the underlying AlGaN substrate $N_D[cm^{-3}]$.

To allow for numerical simulations of AlGaN Schottky diodes, the AlGaN material system as well as the TSB-model were implemented in a physical drift-diffusion simulator (TCAD software). This approach has two advantages: (i) it evades some of the approximations made in the analytical description [16] and (ii) it allows for more complex 2D/3D structures to be simulated. Good fits with the experimental I-V data were obtained for various Schottky diodes (two examples are given in fig. 3).

Concerning the nature of these defects, theoretical calculations [17], [18] have identified Nitrogen vacancies or Oxygen impurities as possible dopants. Another possibility is that impurities are left behind on the AlGaN-surface during processing. A clean with buffered HF could for example leave some fluorine impurities on the surface.

A.4 Tunneling Current in the TSB model

In order to further investigate the current transport in AlGaN Schottky diodes, the tunneling current was also calculated using the formula for current through an arbitrary Schottky barrier, derived by Padovani *et al.* [13] in the 1960's. This general formula is based on a semi-classical quantum mechanical approach:

$$J = \frac{2\pi q m^*}{h^3} \int_0^\infty T(E_x) \int_0^\infty \begin{pmatrix} f_s(E_p + E_x) \\ -f_m(E_p + E_x) \end{pmatrix} dE_p dE_x \quad (2)$$

Following the approach by [19] and using the Wentzel-Kramers-Brillouin (WKB) approximation for the tunneling probability $T(E_x)$ [20], expression 2 was numerically evaluated, starting from an exact analytical expression for the form of the Schottky barrier. This avoids the approximations made in [16].

The shape of the Schottky Barrier is drawn in fig. 4, at four different reverse bias voltages. The transient between the defect-rich TSB-layer and the lowly doped substrate can clearly be distinguished at 4.8 nm. The I-V curve calculated from eq. 2 is plotted in the inset in fig. 5, while the large figure plots the tunneling current in function of the electron energy for the 4 different bias conditions. The latter can be calculated by evaluating eq. 2 except for the integral over dE_x. Two current regimes can clearly be distinguished:

- A TFE-mechanism dominates at small reverse bias: the energy at which electrons tunnel through the Schottky barrier coincides with the boundary between the defect-rich TSB-layer and the AlGaN substrate (fig. 4 and 5). When increasing the reverse bias from -0.1 to -0.6 Volt, two effects can be observed. (i) The Schottky barrier gets thinner (fig. 4), increasing the tunneling probability. (ii) The energy at which the most electrons tunnel through the barrier lowers, as the transient between the TSB-layer and the AlGaN substrate reaches a lower energy value. This also leads to an increase in tunneling current, as more electrons are available for tunneling at lower energies. Both effects working together are responsible the fast increase in leakage current observed at small reverse bias in fig. 5
- At higher reverse bias, a FE-mechanism dominates: the energy at which the electrons are tunneling through the

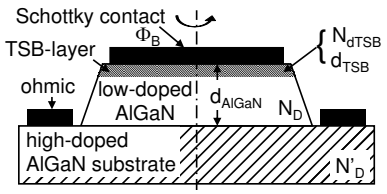

Fig. 6
Device structure of the reference Schottky UV-detector.

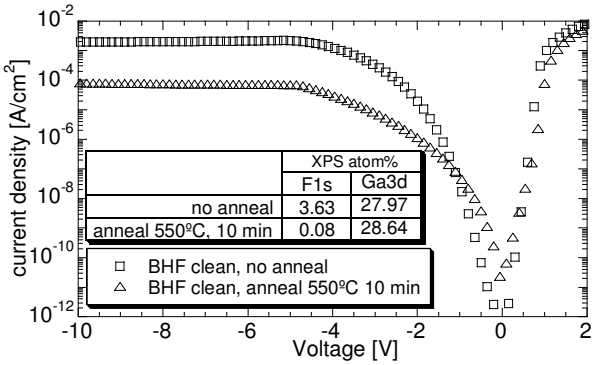

Fig. 7
I-V curves and XPS measurents (inset) for two samples, showing the influence of an anneal before metal deposition.

barrier has been lowered to the Fermi level of the metal. A further increase of the voltage still makes the Schottky barrier thinner but the tunneling-maximum will remain at the metal Fermi level. This can clearly be seen when comparing the curves for -4.5 and -5.0 Volt in fig. 5. The FE mechanism shows a less pronounced voltage dependence, resulting in a flatter I-V curve.

A.5 Theoretical models: conclusion

It can thus be concluded that nor the classical TE model, nor the more advanced TFE/FE model give a good description of AlGaN Schottky diodes, which are considered the primary candidate for UV-detector pixels. The TSB-model, proposed by Hasegawa [16], has been shown to produce good fits. This model has been implemented in a TCAD drift-diffusion simulator together with the AlGaN material system, allowing numerical simulations on arbitrary AlGaN structures. A physical interpretation of the I-V behavior has been further elaborated by evaluating the analytical description given for tunneling current by [13] based on the WKB-approximation.

B. Key issues in technology development

As pointed out in the introduction, reducing the dark current is key to increasing the S/N ratio and thus the performance of AlGaN UV-detectors. This section presents a general analysis, based on the TSB model and TCAD simulations. Its goal is to identify which parameters should be changed to reduce the dark current. Starting from a reference Schottky diode, parameters were changed and their influence on the I-V characteristic investigated. Fig. 6 shows a schematic of the reference diode. It's physical parameters are: $\Phi_B = 1.2eV$, $N_{dTSB} = 4.10^{18}cm^{-3}$, $d_{TSB} = 20nm$, $d_{AlGaN} = 100nm$ $N_D = 4.10^{16}cm^{-3}$, $N'_D = 4.10^{18}cm^{-3}$.

- Increasing the Schottky barrier height (e.g. by using another Schottky metal) by 100 meV results in a factor 15 reduction of the dark current.
- Reducing defect density in the TSB-layer by a factor of 2 reduces the dark current by a factor of about 2000. This huge decrease can be explained by the exponential dependence of the tunneling current through the Schottky barrier on the barrier thickness. Reducing the defect density underneath the Schottky contact thus appears crucial to increased performance.
- Reducing the thickness of the TSB-layer has a similar effect on the I-V curve: making the TSB half as thick reduces the dark current by a factor of 1500.
- The effect of the AlGaN doping level is much less pronounced: a reduction by a factor of 10 only results in a reduction of the leakage current by less than an order of magnitude.
- The thickness of the low-doped AlGaN has a negligable influence on the I-V curve for low reverse bias. At higher reverse bias however, a thicker layer results in reduced leakage current, making this an important design parameter for high-power or high-voltage switching diodes. For UV-detectors however, a low reverse bias is used.
- The doping level of the substrate (serving as an ohmic contact) has no influence on the leakage current. It must be sufficiently high to keep a small series resistance.

The significance of this analysis it that it contains valuable information for process engineering. The key to improving pixel performance is reducing the amount of defects underneath the Schottky contact. Optimized surface cleaning procedures before depositing the Schottky contact, are expected to have a much larger influence than changing the type of metal contact used. Improving the quality of the substrate material or changing layer thicknesses only has a minor influence on the performance.

C. Experimental results

x-ray photoemission spectroscopy (XPS) measurements were performed on two GaN diode-samples before the deposition of the Schottky metal contact. Cleaning of the substrate with buffered HF (BHF) transformed part of the GaN surface into GalliumFluoride. This high surface defect density fits the description given by the TSB-model. On the first sample, the Schottky metal was deposited immediately after the BHF clean. The second sample received an anneal (550C, 10 min.) prior to the metal deposition. The XPS-measurements were performed prior to the metal deposition (inset in fig. 7). They clearly show a reduction of Fluorine at the surface due to the anneal, which succeeds in evaporating most of the Fluorine. The anneal therefore results in a GaN-surface with less Fluorine impurities. From the analysis in section II-B, the annealed sample is

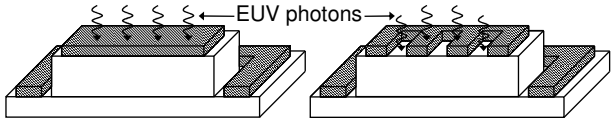

Fig. 8
DEVICE STRUCTURE FOR THE FINGERED AND FULL CONTACT

expected to have lower dark current because of its better surface quality. I-V measurements of both diodes are given in fig. 7 and show a 30x reduction in leakage current. This confirms that improving the surface quality underneath the Schottky contact can result in order-of-magnitude reductions in dark current and supports the analysis given in section II-B.

III. DETECTOR STRUCTURES

Maximizing the photocurrent is the second way to increase the performance of AlGaN EUV-detectors. Where the dark current has been shown to depend mainly on the TSB-parameters, the detector structure is believed to play an important part in the photo current. Section III-A will discuss the use of a fingered Schottky contact. Elaborating on section II, all structures are assumed to have a TSB-layer ($N_{dTSB} = 4.10^{18} cm^{-3}$, $d_{TSB} = 10nm$, $\Phi_B = 1.1eV$). UV-flux density is $100mW/cm^{-2}$ with a wavelength of 180 nm (to allow for comparison with our measurement set-up).

A. Fingered Schottky contact

In order to maximize the photocurrent, a fingered Schottky contact is examined. EUV-photons need to be absorbed in - or close to - the space charge region (SCR) underneath the Schottky contact. There, a generated electron-hole can be separated by the electric field, causing a current flow. When a photon is absorbed outside the SCR, the generated electron hole-pair will recombine after some time and no current flow is observed. Also, photons absorbed in the Schottky metal are lost.

In order to address this loss, a fingered Schottky contact is compared with a full Schottky contact. A schematic of these two structures is given in fig. 8. The full Schottky contact covers the entire semiconductor. Here, the light first has to pass through the metal to give rise to a current. The fingered Schottky contact covers only a certain percentage of the semiconductor surface. This contact looks much like an everyday fork, allowing photons to directly hit the semiconductor surface between the tips, hereby avoiding absorption-losses in the metal.

A.1 TCAD Simulation results

The fingered structure was analyzed using the customized TCAD software discussed in section II. Fig. 9 plots the photo current in the fingered structure, in function of the area effectively covered by the Schottky metal. A finger pitch of 2 μm is assumed. Therefore, 40 % metal coverage corresponds with 0.8 μm wide fingers with a 1.2

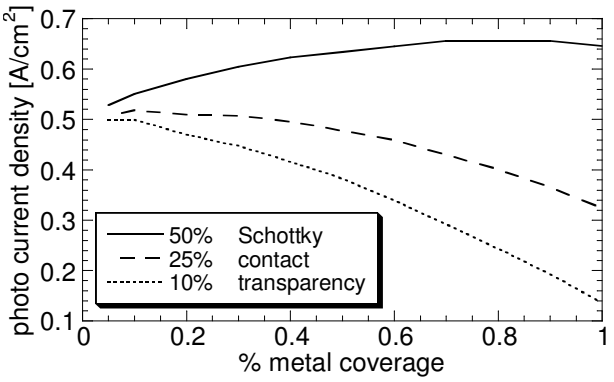

Fig. 9
PHOTO CURRENT FOR A FINGERED SCHOTTKY CONTACT, IN FUNCTION OF METAL COVERAGE AND METAL TRANSPARENCY.

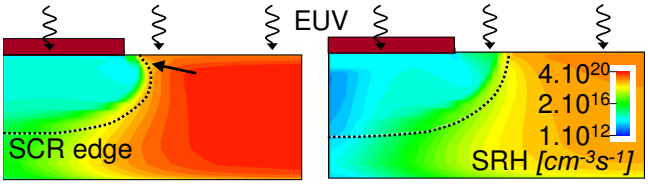

Fig. 10
SRH-RECOMBINATION AND SCR-EDGE AT THE EDGE OF A SCHOTTKY FINGER, WITH (LEFT) AND WITHOUT (RIGHT) TSB. BOTH PLOTS ARE 1 μm WIDE.

μm finger-to-finger spacing. Unlike what can be expected, the fingered structure has lower photocurrent than it's completely covered counterpart (assuming 50% metal transparency). As the Schottky metal gets less transparent, the fingered structure has the highest photocurrent, however the effect remains relatively small.

This effect can be explained by the TSB-model. Fig. 10 shows the Schockley-Read-Hall (SRH) recombination at the edge of such a metal finger. The dashed line represents the edge of the SCR-region. Photons absorbed outside the SCR-region have first to diffuse to the SCR-region in order to generate current. A closer look at the edge of the metal finger marks the effect of the TSB-model: the high defect concentration under the Schottky contact causes the SCR to recede towards the contact. A large fraction of the electron-hole pairs generated between the fingers does not generate current but recombines instead, which can be concluded from the high SRH-recombination between the metal fingers. This is the result of the TSB-region, where the high concentration of defects prevents the semiconductor in between the fingers to be fully depleted. Our own measurements, as well as [15] have shown that the transparency of a 10 nm gold layer often used as a Schottky metal is between 25 and 50 %.

The dark current in these fingered structures suffers from an additional effect. The higher electric field at the edge

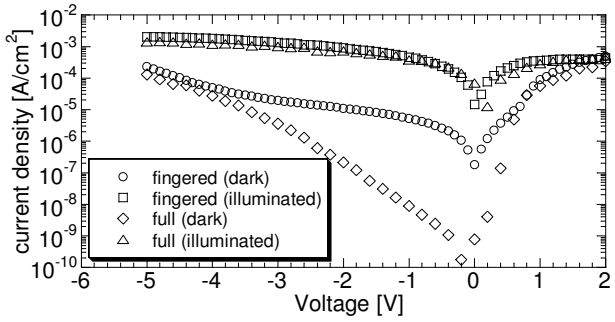

Fig. 11
Experimental I-V curve for a fingered and full Schottky diode: photo and dark current.

of the metal finger, causes the Schottky barrier to become thinner. As the tunneling current increases exponentially with the thickness of this Schottky barrier, the leakage is considerably higher. It is difficult to determine the exact effect on the dark current, as this depends on the detailed morphology of the finger edges. Still, a dark current increase of about 4 orders of magnitude is expected for the fingered contact.

A.2 Experimental results

From the TCAD simulations, it was concluded that the fingered Schottky diode would have the same photo current as a fully covered one, but a much higher dark current. Fig. 11 shows experimental I-V curves for these structures with and without illumination. Both structures were fabricated on the mesa structure depicted in fig. 6, with a diameter of 3 mm. Fingers were 4 μm wide with 4 μm finger-to-finger spacing. The detectors were illuminated with a continuous UV-spectrum with wavelengths ranging from 180 to 400 nm, under identical photon flux. It can be seen that the photocurrent of both structures is very similar, which is in agreement with the performed TCAD simulations. The dark current of the fingered structure however is almost 5 orders of magnitude higher at small reverse bias. This supports the results obtained from the TCAD simulations.

IV. Conclusions

For this study, we implemented TCAD simulations to optimize the performance of III-N EUV-detectors for space applications and advanced lithography tools. Using the customized simulator, the development time and costs of AlGaN EUV-detectors were reduced, as key issues in technology development were successfully identified. For future research, different processing options can first be evaluated through TCAD simulations before starting time consuming experiments.

We show that (i) the high dark current in present AlGaN Schottky diodes can indeed be explained by the Thin Surface Barrier model proposed by Hasegawa *et al.* in [16] for GaN. (ii) This model and AlGaN material parameters were implemented in TCAD software and combined with semi-classical quantum mechanical calculations and experimental results to analyze dark current. (iii) From these simulations, it was concluded that the high dark current in present III-N Schottky diodes is mainly determined by surface defects (TSB defect density N_{dTSB} and TSB thickness d_{TSB}). This was verified experimentally by combining XPS and I-V measurements. Lowering the surface defect density is therefore key to increasing future AlGaN EUV-detector performance, and should be the focus of future technology development. (iv) Finally, a fully covered semi-transparent Schottky contact was shown to provide a good compromise between low leakage and sufficient photocurrent.

Acknowledgments

Acknowledgments were removed for the IEEE Student Paper Contest 2008 (no references to the authors is allowed).

References

[1] X., *Solar Orbiter website*, [Online], Available: http://sci.esa.int/science-e/www/area/index.cfm?fareaid=45, last checked: 2007-10-16
[2] Jean-Franois Hochedez, "New UV detectors for solar observations," *Proc. SPIE*, vol. 4853, pp. 419-426, August 2002.
[3] Richard A. Harrison, "Detector Development Requirements for the ESA Solar Orbiter Remote Sensing Instruments," [Online], Available: http://sci.esa.int/science-e/www/area/index.cfm?fareaid=45, last checked: 2007-10-16
[4] Joseph L. Wiza, "Microchannel plate detectors," *Nucl. Instr. Meth.*, vol. 162, pp. 587-601, 1979
[5] M. Clampin, "Ultraviolet-optical charge-coupled devices for space instrumentation," *Opt. Eng.*, vol. 41, no. 6, pp. 1185-1191, 2002.
[6] Shahid Aslam, "External quantum efficiency of Pt/n-GaN Schottky diodes in the spectral range 5-500nm," *Nucl. Instr. Meth. Phys. Res. A*, vol. 539, pp. 84-92, 2005.
[7] ad-hoc UV-visible Detectors Working Group, "Ultraviolet and Visible Detectors for Future Space Astrophysics Missions: A Report," NASA Office of Space Science, Tech. Rep., 2001.
[8] J. John, "AlGaN focal plane arrays for imaging applications in the extreme ultravioet (EUV) wavelength range," *Proc. SPIE Opt. and Optoelectr., Optical Sensors*, vol. 6585, 658505 (2007)
[9] J. L. Pau, "Response of ultra-low dislocation density GaN photodetectors in the near- and vacuum-ultraviolet," *J. Appl. Phys.*, vol. 95, no. 12, pp.8275-8279, June 2004
[10] E. Monroy, "Assessment of GaN metal-semiconductor photodiodes for high-energy ultraviolet photodetection," *Appl. Phys. Lett.*, vol. 80., no. 17, pp 3198-3200, April 2002
[11] A. Osinsky, "Schottky barrier photodetectors based on AlGaN," *Appl. Phys. Lett.*, vol. 72, no. 6, pp 742-744, February 1998
[12] S. M. Sze, *Physics of Semiconductor Devices 2nd ed.*, John Wiley and Sons, 1981
[13] F. A. Padovani, "Field and Thermionic-Field emission in Schottky barriers," *Solid-State Electron.*, vol. 9, pp. 695-707, 1966
[14] X., *Sentaurus Manual*, Y-2006.06, Synopsys Inc., Jun 2006
[15] M. Razeghi, "Semiconductor ultraviolet detectors," *J. Appl. Phys.*, vol. 79, no. 10, pp. 7433-7473, May 1996
[16] H. Hasegawa, "Anomalous current transport in n-type GaN," *J. Vac. Sci. Technol. B*, vol. 20, no. 4, pp. 1647-1655, Jul/Aug 2002
[17] P. Boguslawski, "Native defects in gallium nitride," *Phys. Rev. B.*, vol. 51, no. 23, pp. 17255-17259, June 1995
[18] T.L. Tansley, "Point-defect energies in nitrides of aluminum, gallium and indium," *Phys. Rev. B.*, vol. 45, no. 19, pp. 10942-10950, May 1992
[19] J. Kotani, "Analysis and control of excess leakage currents in nitride based Schottky diodes based on thin surface barrier model," *J. Vac. Sci. Technol. B*, vol. 22, no. 3, pp. 2179-2187, Jul/Aug 2004
[20] E.H. Rhoderick, *Metal-Semiconductor Contacts*, Oxford Science Publications, 1988